

Achieving operational two-way laser acquisition for OPALS payload on the International Space Station

Matthew J. Abrahamson^{*}, Bogdan V. Oaida, Oleg Sindiy, Abhijit Biswas
Jet Propulsion Laboratory, California Institute of Technology,
4800 Oak Grove Drive, Pasadena, CA 91109

ABSTRACT

The Optical PAYload for Lasercomm Science (OPALS) experiment was installed on the International Space Station (ISS) in April 2014. Developed as a technology demonstration, its objective was to experiment with space-to-ground optical communications transmissions from Low Earth Orbit. More than a dozen successful optical links were established between a Wrightwood, California-based ground telescope and the OPALS flight terminal from June 2014 to September 2014. Each transmission required precise bi-directional pointing to be maintained between the space-based transmitter and ground-based receiver. This was accomplished by acquiring and tracking a laser beacon signal transmitted from the ground telescope to the OPALS flight terminal on the ISS. OPALS demonstrated the ability to nominally acquire the beacon within three seconds at 25° elevation and maintain lock within 140 μ rad (3σ) for the full 150-second transmission duration while slewing at rates up to 1°/sec. Additional acquisition attempts in low elevation and weather-challenged conditions provided valuable insight on the optical link robustness under off-nominal operational conditions.

Keywords: OPALS, optical communications, lasercomm, ISS, OCTL, acquisition, tracking

1 INTRODUCTION

During summer of 2014, the Optical PAYload for Lasercomm Science (OPALS) demonstrated space-to-ground optical communications transmissions from an external platform on the International Space Station (ISS) using a 2.5W, 1550-nm laser. The transmissions were received and digitally stored for post-processing decoding³ at the Optical Communications Telescope Laboratory (OCTL) ground station near Wrightwood, California at data rates up to 50 Mbps. These transmissions included high-definition videos, text files, pseudo-random bit sequences (PRBS) with PN 8, and payload-generated engineering data. The 1.08-mrad beamwidth of the downlink laser signal was pointed successfully at the ground-based receiver by acquiring and tracking a 1.5 mrad beacon uplinked from the ground. This paper discusses the operational challenges of establishing bi-directional pointing alignment and maintaining it under various pass conditions.

The OPALS bi-directional pointing acquisition strategy relies on a 976-nm laser beacon transmitted from a ground telescope to the ISS. A flight-based camera with an 8 nm bandpass filter centered at 976 nm identifies the beacon signal and steers the downlink beam toward the ground-based receiver. This acquisition strategy relies on adequate beacon signal in the presence of additive background noise and transient disturbances. The background level was found to vary widely depending on the Sun geometry at the transmitter and receiver during each attempt. For each pass, a camera exposure time and a signal threshold level were chosen based on the predicted lighting conditions. During OPALS prime mission, the threshold setting choice during daytime passes was challenged by the background distribution uncertainty on the wide field-of-view camera, the unpredictability of clouds or glint caused by near specular reflection, the relatively wide bandpass spectral filter, and the limited dynamic range of an 8-bit CCD camera. Despite these challenges, the daytime beacon signal was acquired and tracked most of the time, though on cloudy days and in the presence of transient specular reflection interesting artifacts were observed. With the implemented onboard control algorithm, low threshold settings were found to increase link interruption frequency, while high threshold settings were found to reduce the probability of beacon signal lock. This paper discusses the challenges of the acquisition strategy implemented during OPALS operations.

^{*} Corresponding author: Matthew.Abrahamson@jpl.nasa.gov; Phone: (818)-354-2880; Mail: 4800 Oak Grove Dr., M/S 301-121, Pasadena, CA 91109

2 CONCEPT OF OPERATIONS

OPALS is a low-cost, technology demonstration mission for optical communications in LEO. It was developed by the Jet Propulsion Laboratory to experiment with space-to-ground optical links. It is composed of a Flight System (FS) integrated on the ISS, a Ground System (GS) incorporated at the OCTL telescope, and Mission Operations System (MOS) located at JPL⁴. The MOS, in coordination with the NASA Marshall Space Flight Center’s Huntsville Operations Support Center (HOSC), remotely executes real-time FS operations while a small operations staff at the OCTL telescope executes supporting GS operations¹. The generous mass, power, and volume allocations offered by the ISS allowed the FS to be primarily composed of low cost, Commercial, Off-The-Shelf (COTS) components, many of which are housed within an air-cooled, pressurized, sealed container on orbit.

Space-to-ground transmission opportunities occur when a clear line of sight exists between the flight terminal and ground receiver. This is defined as the “Demonstration Window” and typically lasts a maximum of 150 seconds due to the ISS orbital path, laser pointing constraints from ISS obstruction, and the nominal 25° elevation acquisition. For low elevation acquisitions, this transmission time was extended to 250 seconds. Figure 1 illustrates the OPALS concept of operations within the Demonstration Window. At the start of the window, the GS illuminates the ISS with a 976-nm laser beacon as it rises above the horizon. The beacon pointing is maintained using 10 Hz pointing predictions generated from ISS GPS coordinates¹. By using open loop pointing at the GS, OPALS is able to execute transmissions at all times of the day, and thus does not require the ISS to be sunlit, which is needed to enable optical tracking.

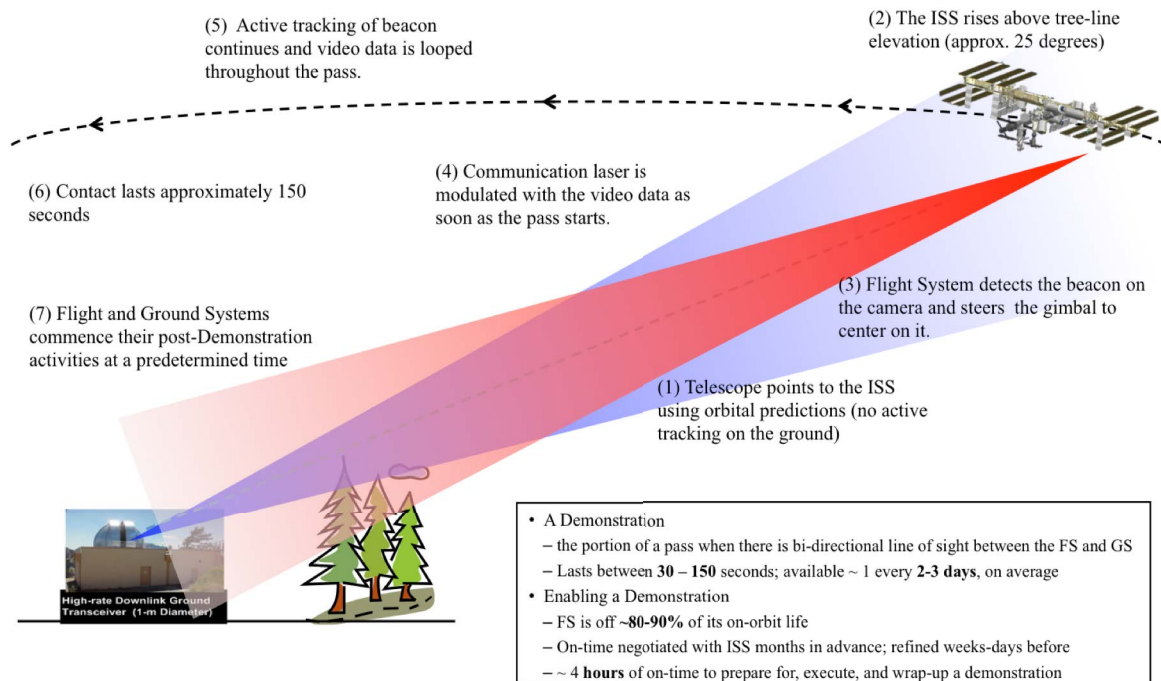


Figure 1: The OPALS concept of operations during the 150-second Demonstration period, when a clear line of sight exists between the flight and ground terminals.

The FS attempts to acquire the beacon signal using a charge-coupled device (CCD) camera with a narrowband 976 nm filter mounted on a two-axis gimbal. It begins the beacon search by following a coarse pointing profile at a predetermined acquisition start time (nominally, when the ISS is 25° elevation above the horizon). The camera processes frames at a rate of 100 Hz to detect a valid beacon signal on the 640 × 480 pixel focal plane. When the beacon signal exceeds a set detection threshold, the FS gimbal drives the signal to the CCD center using a Proportional-Integral (PI) control algorithm. Due to the co-aligned configuration of the bistatic FS optical transmit and receive paths, the downlink laser is pointed back to the GS receiver as long as the beacon signal is centered on the CCD.

A successful acquisition occurs if the onboard control algorithm successfully centers and retains the beacon sufficiently well for the downlink beam to remain on the ground receiver. Since the downlink beam divergence angle is approximately 1.08 mrad, the beam cannot be off-pointed by more than half of that, the equivalent of 2 camera pixels.

The ISS serves as an excellent platform for a LEO link demonstration. It orbits in a near circular orbit at an altitude of approximately 400km above the Earth. With an orbital period of 90 minutes and an inclination of 51.6°, the ISS provides global access on a relatively short time scale. For ground sites in the mid-latitudes, the ISS will fly overhead twice daily with one southwest to northeast ascending pass and one northwest to southeast descending pass.

OPALS is mounted on an external platform called the Express Logistics Carrier-1 (ELC-1) that provides mechanical, electrical, and data interfaces to the ISS as well as a nadir view of the Earth⁴. Due to pointing constraints levied by ISS Keep Out Zones, OPALS opportunities for transmission occur once every two days on average¹. During a nominal 150-second transmission, the range varies from 850 km at 25° elevation to near 400 km at zenith, with corresponding gimbals slew rates of 0.5°/s to 1.0°/s, primarily in the azimuth axis, to compensate for the ISS orbital motion. Figure 2 illustrates the orientation of OPALS on ELC-1, with a nadir-facing optical transceiver mounted on a two-axis gimbal. The OPALS electronics are stored behind the optical transceiver in an air-pressurized sealed container⁴.

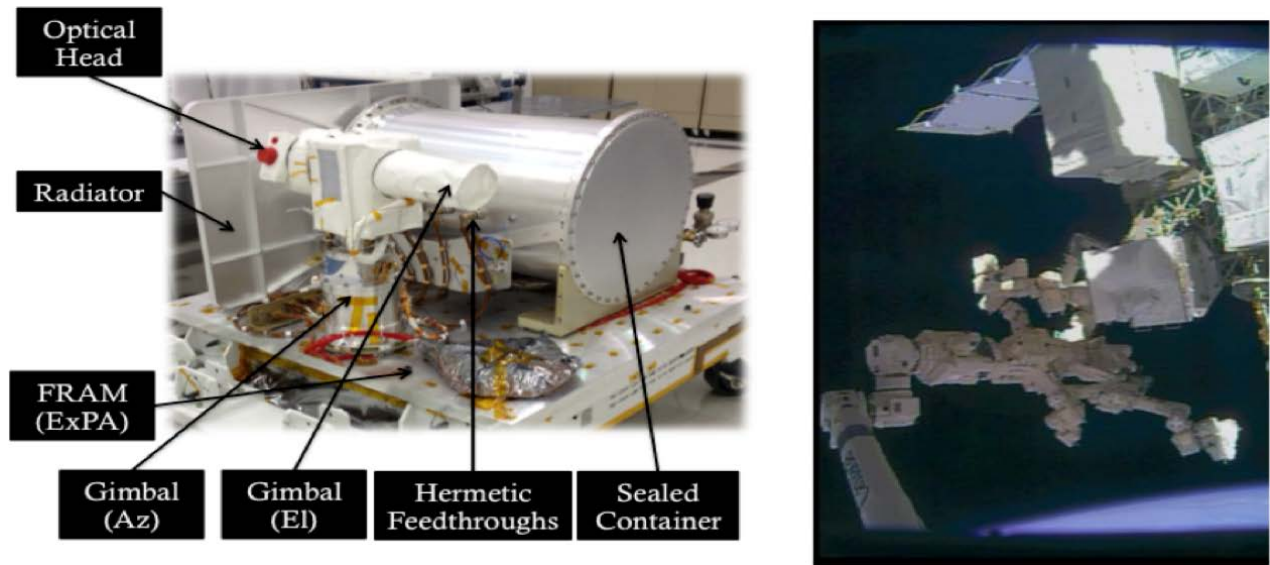


Figure 2: The OPALS Flight System in the laboratory (left) and on orbit (right). It is composed of an optical transceiver mounted atop a two-axis gimbal and an air-pressurized sealed container housing COTS electronics.

3 BEACON DETECTION, ACQUISITION AND TRACKING STRATEGY

The first step in achieving a successful downlink is locking onto the ground beacon with the FS optical transceiver. This acquisition process occurs in two phases: open-loop tracking, followed by a transition to closed-loop tracking.

3.1 Ground beacon overview

The OPALS GS was built within the existing OCTL telescope at the Table Mountain Observatory in Wrightwood, California. The telescope includes a 1-meter diameter primary mirror and uses an azimuth-elevation mount capable of tracking LEO to deep-space objects. The implemented GS architecture features a mono-static uplink and downlink path through the common 1-meter aperture. The telescope was retrofitted with an optical transceiver assembly capable of transmitting a 976 nm beacon while receiving 1550 nm downlink.

Figure 3 provides an optical schematic view of the optical transceiver coupled to the coude path of the telescope. The OPALS GS optical transceiver is coupled to the telescope with an off-axis parabola (OAP) placed at the telescope coude focus. The transmitting and receiving optical paths are separated by the dichroic beam-splitter, which reflects the beacon to the OAP while passing the downlink signal to the fast steering mirror. The fast steering mirror is used to stabilize the line of sight of the downlink signal on the communications detector while the telescope is slewing to track the ISS. A

3nm bandpass 1550nm spectral filter was used in front of the indium gallium arsenide (InGaAs) acquisition camera and avalanche photodiode (APD) detector in order to block backscattered beacon signal as well as sky radiance during day passes.

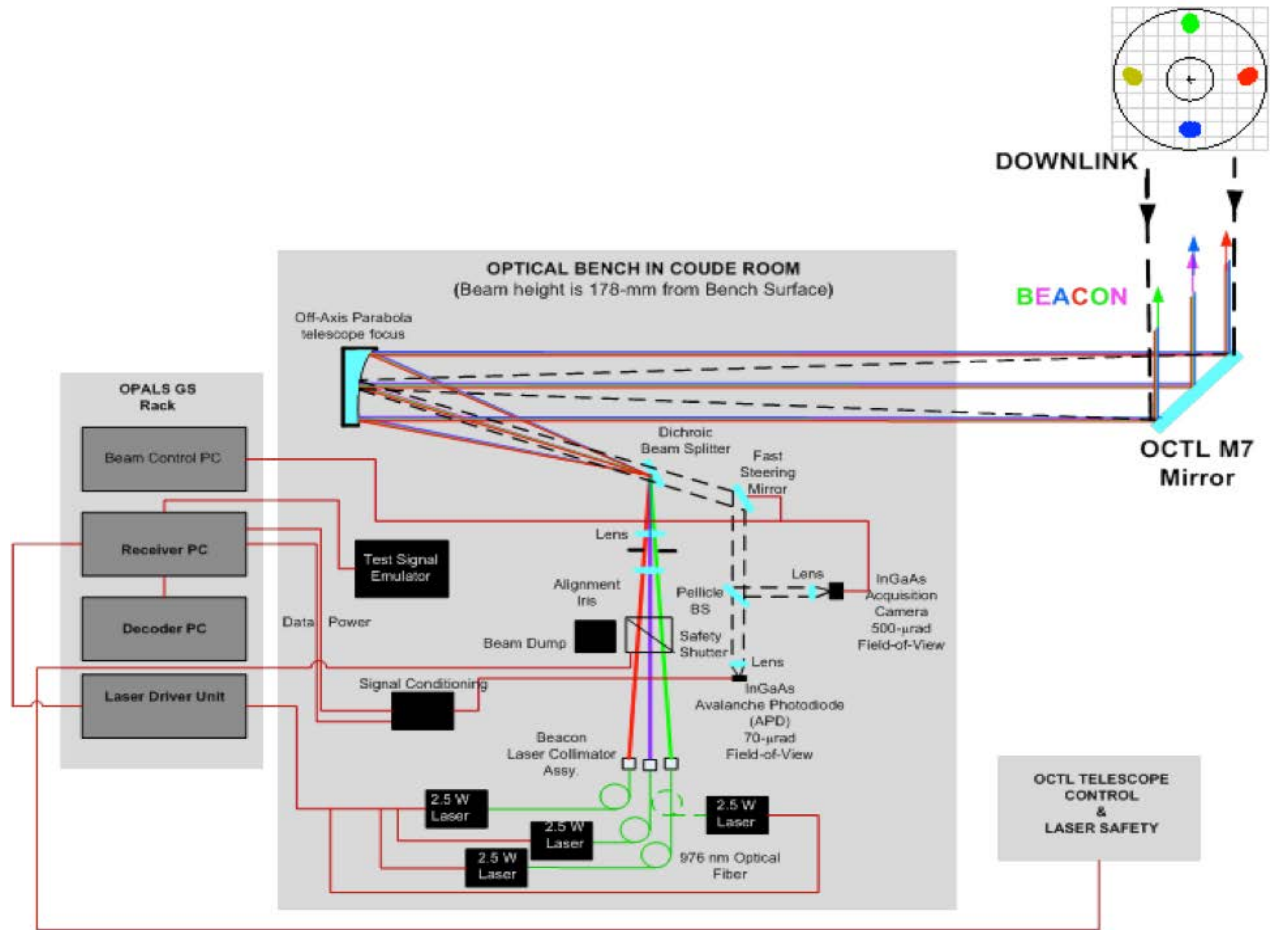


Figure 3: The OPALS GS housed within the OCTL telescope at the JPL Table Mountain Facility.

Free-space optical communications requires high-accuracy pointing to maintain line of sight between transmitter and receiver terminals. In all free-space optical communications demonstrations from space, this has been accomplished by beacon tracking. The OCTL beacon wavelength of 976 nm provides optical isolation from the transmit wavelength (1550 nm), easing implementation at both ends of the link.

The beacon is comprised of four mutually incoherent, 2.5W fiber coupled multimode laser beams to achieve spatial diversity gain and reduce scintillation at the flight-terminal aperture. The four collimators are spatially arranged in a diamond pattern so that all beams are focused and overlapped at the focus of the OAP. This results in the beams being projected out of the telescope as sub-aperture beamlets as shown by the different colored spots on the primary mirror in Figure 3. The large beam divergences (1 to 1.5 mrad) of the beacon lasers coupled with the relatively modest powers (approx. 1 W exiting the aperture) did not require laser safety inhibits for aircraft safety because of the NOHD (Nominal Ocular Hazard Distance) being a few tens of meters from the exit aperture. Predictive avoidance (PA) needed from the United States Air Force (USAF) Laser Clearing House was waived for similar reasons.

3.2 Open Loop Tracking

With the fast-changing viewing geometry within a pass, the FS optical transceiver must be blind-pointed to the ground beacon location and vice versa. This is very much akin to RF systems where the downlink antenna is pointed at the receiver according to a pre-computed pointing profile. The OPALS equivalent is called a blind pointing table (BPT), which is uplinked to the FS a few hours prior to each pass. Unlike most satellites, the ISS is subject to high levels of

acceleration disturbances and thus its trajectory is more challenging to predict days in advance to the degree of accuracy required by OPALS, which was on the order of 100 meters for beacon pointing and 1.0 km for FS pointing¹. Due to the wide field-of-view FS camera, the BPT pointing accuracy requirement was more relaxed than the beacon pointing requirement. As Figure 4 shows, the BPT trajectory prediction errors are less than 100 meters within 45 minutes of its generation (OCTL pointing requirement) and less than 1.0 km within 6 hours of its generation (FS pointing requirement). In addition, the ISS attitude uncertainty is on the order of a few degrees due to misalignment, flexing, and controller oscillations⁶. While this was a prime reason for selecting a wide field-of-view camera, in practice the attitude knowledge was generally much better than anticipated.

The BPT is generated on the ground using an ISS GPS state vector and attitude quaternion. The state vector is propagated through the Demonstration period using high-fidelity dynamics models to account for higher order gravitational effects and atmospheric drag, while the attitude is assumed to be a constant offset relative to the local vertical / local horizontal (LVLH) orientation. Because the attitude oscillates with a period equal to the ISS orbital period, the quaternion is sampled an integer multiple of orbits prior to the Demonstration¹. The BPT must be accurate enough to capture the beacon signal within the camera field of view but is not expected to center the downlink beam on the ground receiver.

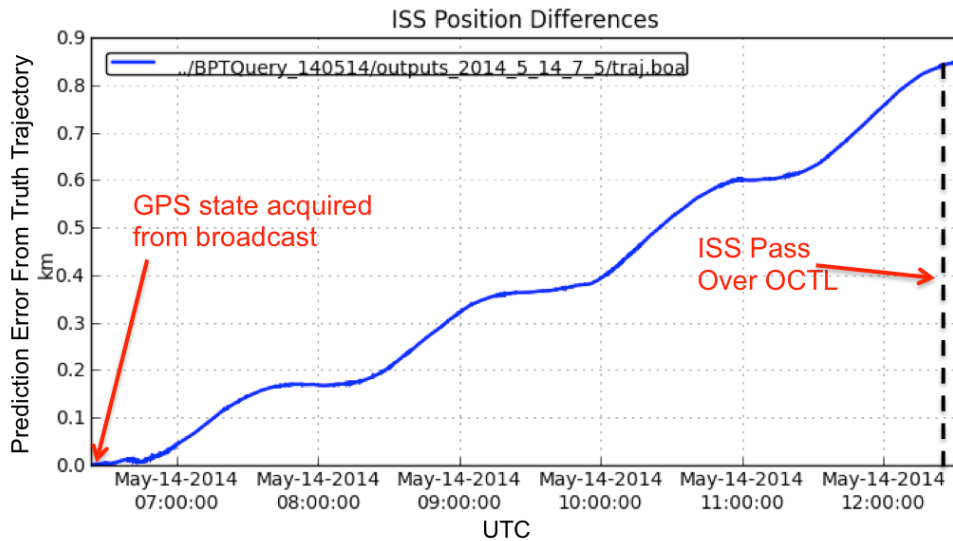


Figure 4: BPT prediction errors as a function of time following generation. ISS trajectory predicts had to be updated 3-6 hours prior to an overpass in order to meet the FS open-loop pointing requirements and within 45 minutes of an overpass to meet GS open-loop pointing requirements.

Aside from ISS prediction errors, the need for a highly accurate BPT was also driven by OPALS' lack of gimbal actuator encoders, which challenged the FS' ability to maintain high-confidence pointing knowledge throughout a transmission. Four electrical limit switches at the ends of the gimbal travel provided the only pointing feedback to the OPALS software. Thus the gimbal relied on dead reckoning during the acquisition process and the gimbal pointing angles reported by the software were based on commanded, rather than executed, values. This approach worked well as long as the gimbal was not subjected to sudden acceleration corrections by the control algorithm, which invariably led to loss of pointing calibration. As will be discussed in section 5.4, this phenomenon often occurred when background optical noise caused rapid switching between tracking targets and in those occurrences impaired the FS's ability to autonomously re-acquire the ground beacon if a loss of signal occurred.

Several minutes prior to each pass, the gimbal pointing was fixed to the first entry of the BPT. When the pre-determined Demonstration time was reached, the gimbal initiated an open-loop drive profile dictated by the position entries in the table. Since the Demonstration time was intended to coincide with the time the beacon neared the center of the CCD, the beacon signal was often seen crossing the CCD a few seconds prior to the gimbal commencing its open-loop drive. Thus

if a good predict was achieved, the system would only spend fractions of a second in open loop prior to transitioning to closed loop, assuming that the signal was above the beacon detection threshold specified for that pass.

3.3 Beacon Detection and Acquisition

The challenge of beacon acquisition involves identifying the true signal from the background noise across a wide range of illumination conditions. Success depends on identifying the correct combination of camera frame exposure and beacon detection threshold for the illumination geometry specific to each pass. Camera frames are processed at 100 Hz and thus the maximum exposure of each frame is 10 milliseconds. The threshold can be thought of as the ceiling for the background noise and thus is effectively the floor for the minimum required signal to declare that a beacon has been found. The OPALS link was designed to operate primarily during low-background conditions, which are most easily achieved when the ground station is in eclipse, due to concerns that the background would be too strong during daytime conditions to enable reliable acquisition and tracking³.

The OPALS FS uses a Commercial Off-The-Shelf (COTS) camera with a CCD detector sensitive in the visible portion of the electromagnetic spectrum and thus has very low Quantum efficiency (approximately 1%) at 976nm. A narrow-band filter blocks transmission outside the 972–980nm range. Each pixel returns an 8-bit Data Number (DN) that is proportional to the number of photons detected.

Once entering the camera aperture, the light is focused on the CCD with a spatial resolution of 262 μ rad per pixel. The design required that 75% of the beacon energy be captured over an area no larger than 16 pixels. The performance was substantially better, with more than 75% of the energy often being captured within an area of 4–6 pixels. During daytime operations, the limited dynamic range of the camera restricted the useful beacon information to 2–4 pixels.

As the system initiates open loop pointing, an onboard algorithm processes each 100Hz camera frame to compute a beacon centroid value. The algorithm:

1. Identifies the brightest pixel found in the 640 x 480 frame
2. Performs a simple center-of-mass calculation to establish the coordinates of the spot
3. Computes the average signal value from the pixels circumscribing an 8 x 8 subframe centered on the spot as the image background level
4. Sums the total DN flux across the 64 pixels in the subframe
5. Subtracts the background level from the total flux to determine the beacon flux

If the signal exceeds the preset beacon detection threshold then the beacon is declared as found, and the system can transition to closed-loop tracking. Otherwise, the system remains in open-loop tracking until a valid signal is detected. This process is repeated in subsequent frames to maintain knowledge of the beacon centroid location for continued closed loop tracking. The results from one frame are shown in Figure 5.

This approach, while simple and easily implementable, has some limitations, many of which were experienced during operations. For example, since the algorithm is only looking for the brightest pixel, if a signal stronger than the actual beacon is detected, the algorithm locks on to it even if the signal signature, that is to say, its shape, is not consistent with that of a beacon. This and other limitations experienced in operations will be discussed in section 4 of this paper.

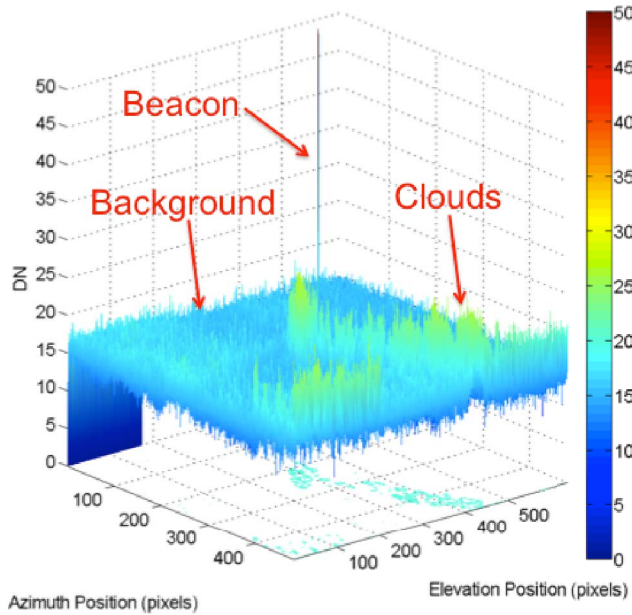


Figure 5: Post-processing of one camera frame shows the beacon signal relative to the background level. In this frame, clouds are seen as being brighter than the cloud-free background. The signal is expressed in DN and measured from 0 to 255.

3.4 Closed Loop Tracking

Once a beacon signal is identified, the proportional-integral (PI) controller commands the gimbal to move the beacon to the center of the CCD pixel array (240, 320) and maintain it there. Following each camera frame, the controller calculates a gimbal correction velocity based on the feedback angular tracking error represented in camera pixels.

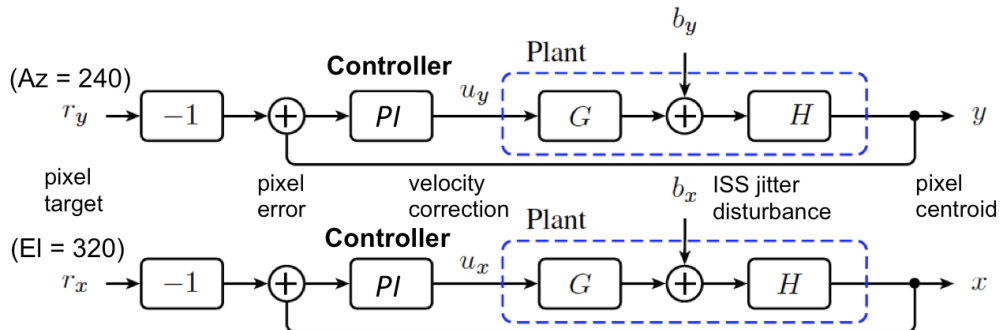


Figure 6: The OPALS control loop diagram detailing gimbal commanding based on camera feedback. The target coordinates are typically (240, 320), but they are adjustable. The block G represents the gimbal dynamics, while the block H represents the camera centroid measurement.

The steady-state residual angular error thus provides a very good proxy for computing the pointing jitter². As long as the beacon signal is above the detection threshold, the system remains in closed-loop tracking. For signals below the threshold, the controller can issue no velocity update. If the signal falls below the threshold for 2 continuous seconds, the beacon is declared lost and the system reverts to open-loop tracking. Since the BPT entries are timestamped, the gimbal reverts to the predicted pointing profile coordinates at the current time, giving it the best chance to reacquire. Figure 7 shows results from a pass on July 15 where clouds caused the temporary loss of beacon signal (same pass as the image in Figure 5) and transition back to open loop on two separate occasions, at 23 and 41 seconds after the start of the pass.

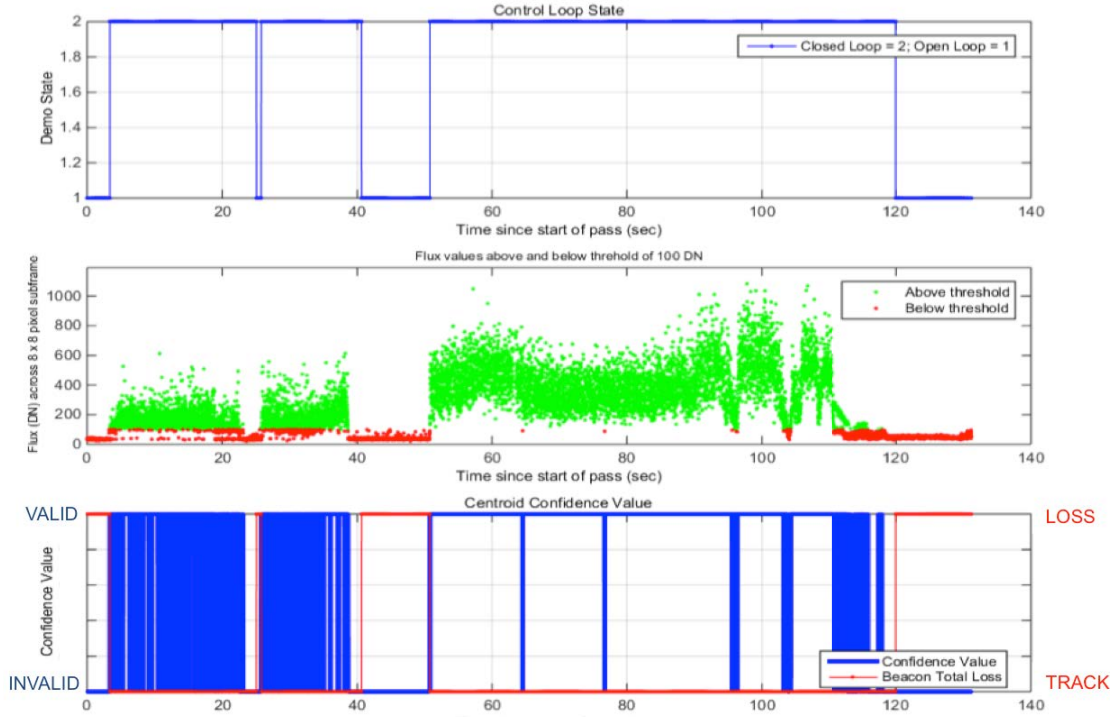


Figure 7: Control loop tracking state (top), recorded beacon flux (middle), and beacon validity flag (1=valid, 0=invalid) with total loss indicator (bottom) for July 15 pass. On this occasion, total beacon loss occurred three times due to the presence of clouds, resulting in transitions to open loop pointing. Total loss occurs when a valid beacon is not detected for 2 consecutive seconds. On the first two losses, the beacon was successfully recovered.

4 NOMINAL ACQUISITION SCENARIOS

The nominal conditions for acquisition occur when the ISS is located at 25° elevation above the western horizon at a range of approximately 850 km from the OCTL receiver. Since the beacon signal-to-noise ratio is higher during night passes, the first nominal acquisitions were planned during nighttime flyovers to increase chances of acquisition success.

4.1 Open loop commissioning

The first acquisition attempt, the Open Loop Characterization Test, was a one-way test that involved the ground beacon only. This test measured the ability to detect the GS beacon on the FS camera and its success was dependent on the open loop tracking capabilities of both the GS telescope and FS gimbal. For this test, the closed loop tracking capability was disabled and a camera exposure time of 1ms was used.

The first successful beacon detection occurred during a May 14, 2014 test at 12:25 UTC, while the ISS was illuminated but OCTL was in eclipse. The pointing sequence initiated when the ISS was 40° in elevation above the western horizon and continued for a duration of 103.1 seconds. The higher elevation acquisition was chosen to increase the angular separation between the FS camera and the rising Sun on the eastern horizon to just over 30° . The ground beacon was toggled on and off at 5 second intervals throughout the pass to uniquely identify the beacon from other potential background signals that might be picked up by the camera.

Figure 8 shows the 8-bit DN value of the brightest FS camera pixel during the pass as well as the recorded flux within the 8×8 subframe. During the period immediately preceding the 12:25:31 GMT sequence start, the flight camera orientation was fixed to the first coordinate in the BPT. The maximum camera pixel was fully saturated by background noise with a DN value of 255 about 90 seconds prior to the sequence start, likely due to stray light from the rising Sun. The observed background level decreased at a rate of 40 DN per second prior to detection of the beacon signal about 5 second prior to the sequence start. From first detection of the beacon through the end of the pointing sequence, the

beacon signal was observed at 5-second intervals with the maximum pixel saturated. The background level decreased at a more rapid pace as the pointing sequence turned the camera away from the eastern horizon.

Similarly, the recorded flux was initially observed at a level of 400-600 DN, increasing to 1200-1800 DN near zenith. Large, short-term variations on the order of ± 100 were observed in the beacon flux. The background flux was observed to be no higher than 75, therefore a beacon detection threshold of 100 was chosen for future acquisition attempts.

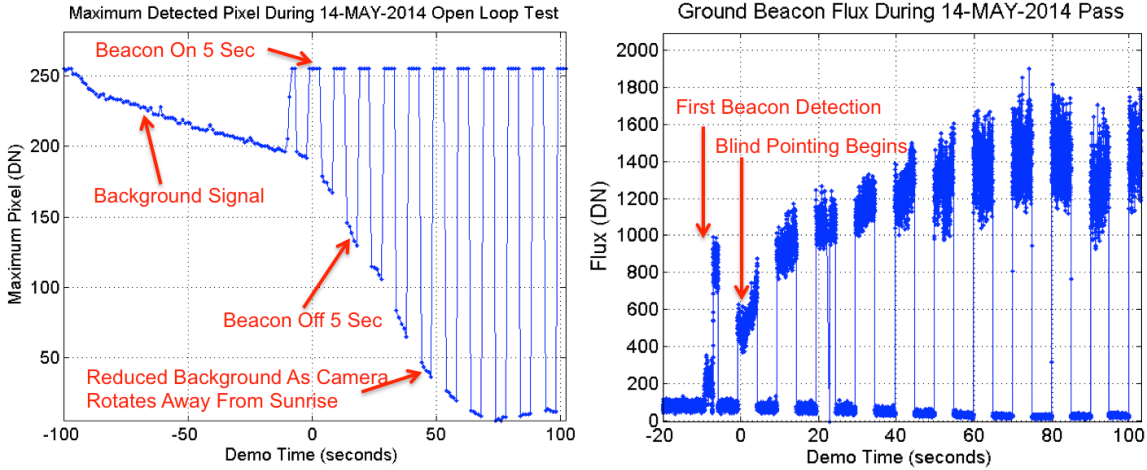


Figure 8: Maximum recorded pixel value (left) and beacon flux (right) during May 14 open loop commissioning test.

Figure 9 shows the deviations of the maximum camera pixel from the CCD center. During the execution of the pointing sequence, the beacon remained within 50 pixels of the CCD center in azimuth and 200 pixels of the CCD center in elevation. The elevation pointing was perturbed more than normal, since a simple LVLH attitude model was used to generate BPT predictions for this pass. The test was an important success since it demonstrated that the beacon signal-to-noise ratio (SNR) and open loop pointing performance were sufficient to support an acquisition at any time during the pointing sequence execution.

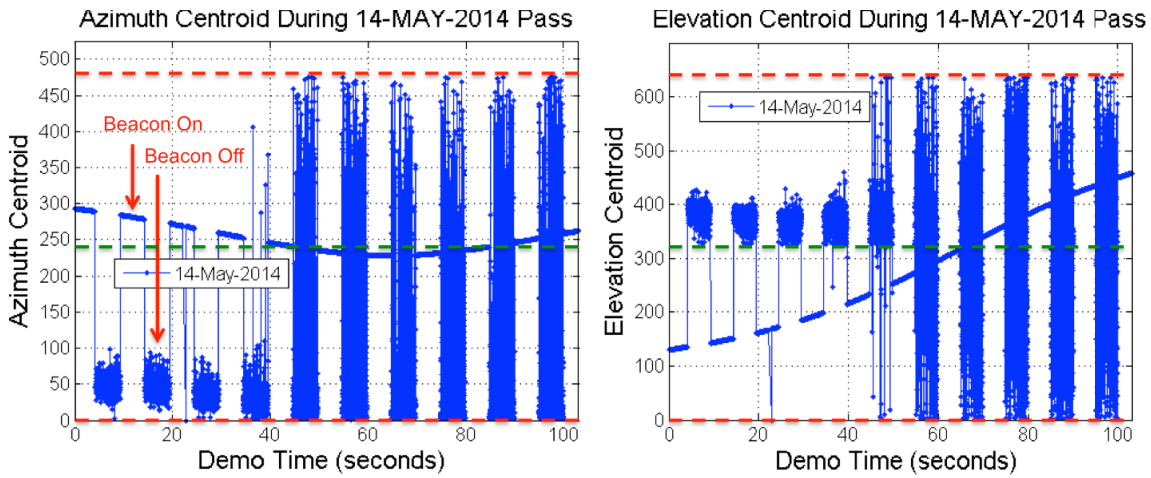


Figure 9: Azimuth (left) and elevation (right) pixel coordinates of maximum signal on the OPALS camera CCD during May 14 open loop commissioning test.

4.2 Closed loop commissioning

The next test, the Closed Loop Commissioning Test, was the first to demonstrate the FS ability to lock onto the beacon and track it for the duration of an entire pass. The first attempt was made on May 25th, 2014 at 8:19:00 UTC while the ISS and OCTL were in eclipse. Unlike the Open Loop Commissioning Test, initial acquisition was attempted at the nominal 25° elevation above the horizon due to a lack of Sun constraints.

With the gimbal pointed almost 60 degrees forward of nadir, at the first location of the BPT, the camera picked up the beacon signal a few seconds prior to pointing sequence initiation as it moved into the CCD center, as shown in Figure 10. The two lines on the plot represent the azimuth and elevation coordinates of the beacon on the camera CCD, with (240, 320) representing the center of the CCD and the desired location for optimal tracking.

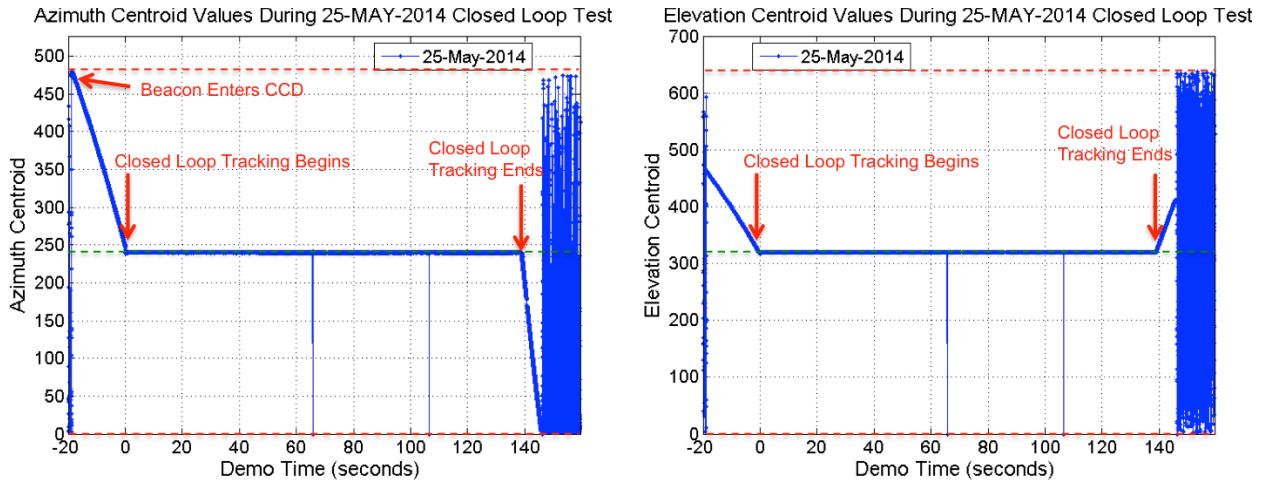


Figure 10: Pixel coordinates of maximum signal on the OPALS camera CCD during May 25 closed loop commissioning test. With good pointing predicts the beacon is visible to the camera before it enters open loop tracking and thus enables a quick transition to closed loop once the Demonstration period begins.

Quick acquisition and transition to closed loop was enabled by the strong beacon signal registered on the camera, as shown in Figure 11.

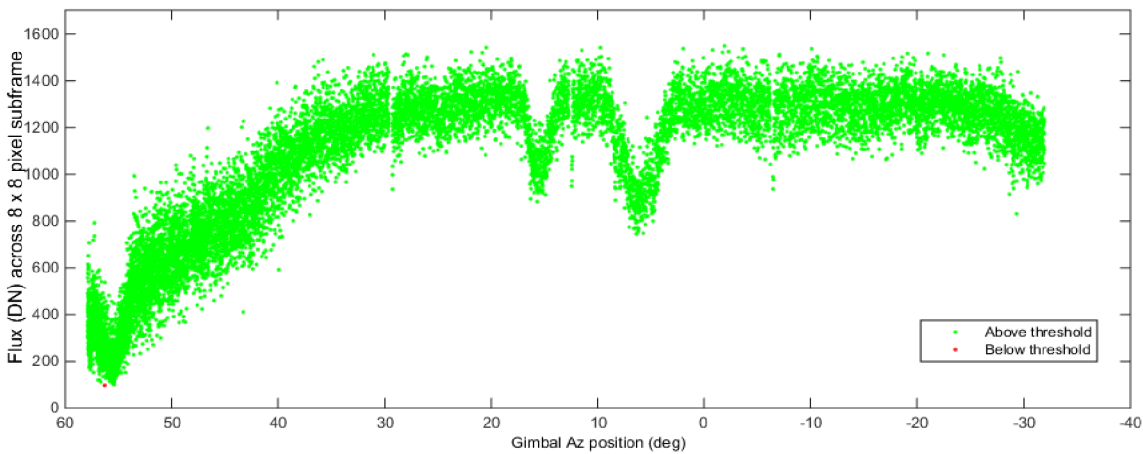


Figure 11: Beacon flux recorded within the 8 x 8 pixel subframe. The beacon signal was very strong for the entire duration of the pass with only one frame registering a flux below the preset threshold of 100 DN. Gimbal azimuth position of zero corresponds approximately to nadir pointing.

For this pass, the camera exposure time was 1ms and the detection threshold was set to a flux of 100 DN, which was exceeded for all but one frame. The recorded flux varies from approximately 200 DN at initial acquisition to 1400 DN near zenith. At least three dips in the recorded beacon flux were observed when the OCTL telescope secondary mirror support struts briefly occulted one of the four laser beacons, thus temporarily reducing the transmitted beacon power. The strong signal also enabled the centroid algorithm to maintain good lock, with the residual tracking errors typically less than 0.2 pixels, as shown in Figure 12. This corresponded to a pointing jitter of approximately 140 μ rad, 3σ , well within the requirement of 375 μ rad, 3σ .

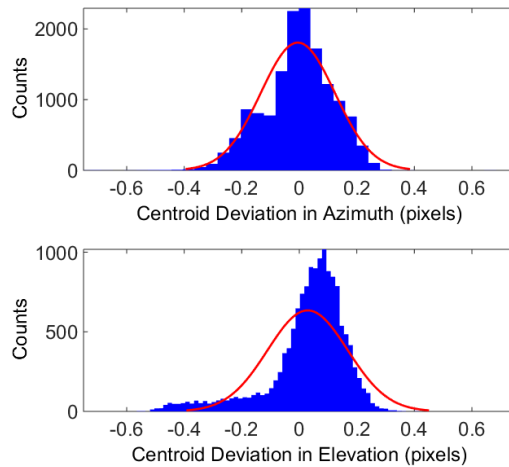


Figure 12: Distribution of centroid error residuals along each axis while in closed loop. This performance corresponds to a jitter of about $140 \mu\text{rad}$, 3σ .

4.3 Mission Success Transmission

The official attempt for achieving OPALS mission success was conducted on June 5, 2014, shortly after sunset at OCTL. The OPALS FS successfully established an optical link within three seconds of the 03:22:03 UTC Demonstration start time and maintained bi-directional pointing throughout the planned 148-second transmission. The FS immediately detected the beacon signal and successfully transitioned to closed loop tracking at the planned 25° elevation angle (as observed from OCTL GS). The initial beacon error at the Demonstration time was only 10 pixels in the azimuth axis and 2 pixels in the elevation axis, allowing the control system to quickly center the beacon within minimal overshoot. A “Hello, World!” video message⁵ was successfully transmitted and reconstructed at the OCTL GS with bit error rates less than 10^{-5} . With the 50 Mbps optical downlink rate, multiple copies of the 175 Megabits message were received by OCTL. Figure 13 provides a still camera frame of the optical signal recorded by the OCTL telescope tracking camera through the main scope.

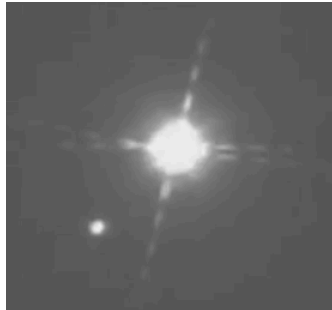


Figure 13: A cropped still camera frame of the infrared optical downlink signal received at OCTL during June 5 optical link demonstration.

As shown in Figure 14, several beacon points were rejected by the onboard control algorithm during initial acquisition due to conservative exposure time and beacon threshold settings for the pass (i.e., exposure time of 0.2 ms and flux beacon threshold of 100). These settings were chosen due to illuminated conditions on the ISS during the sunset pass. Initially, 65-80% of the beacon points were registered as valid, increasing to 100% by 40 seconds into the pass as the OCTL range decreased. There was no detectable degradation in the closed loop tracking performance from the rejected beacon points, indicating sufficient information from the valid points to maintain lock.

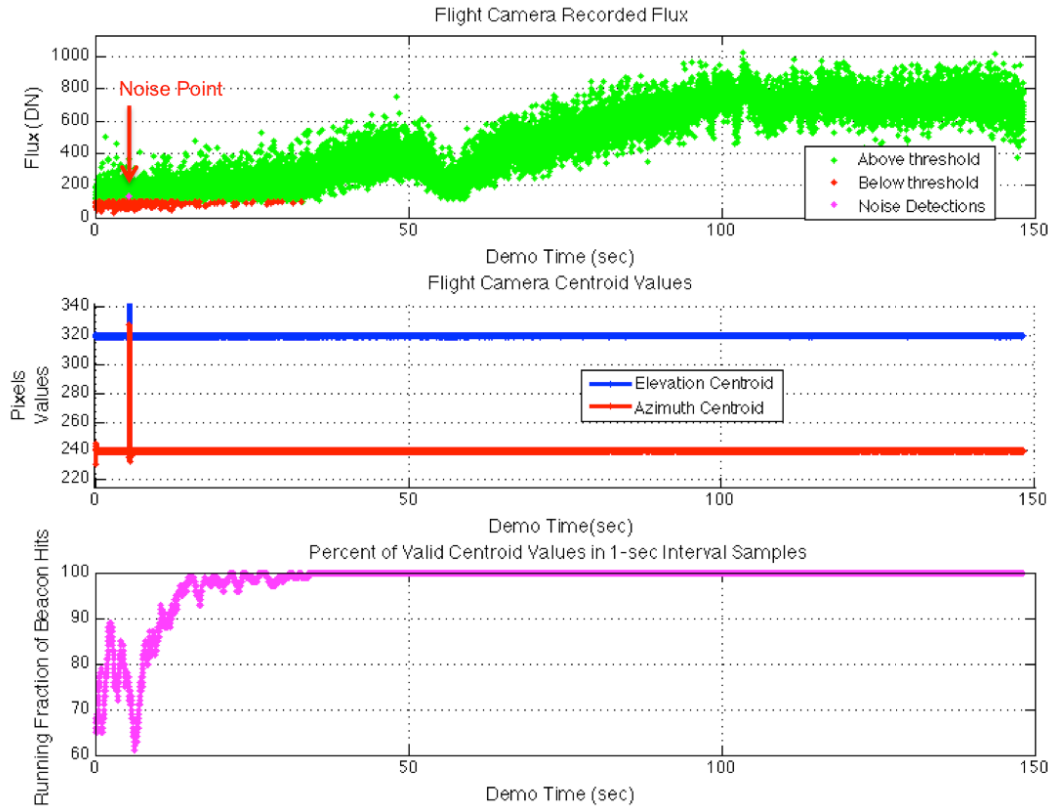


Figure 14: Recorded beacon flux (top), camera centroid coordinates (middle), and beacon validity percentage (bottom) for the 05-JUNE-2014 pass. For the first 40 seconds, several beacon points were rejected due to overly conservative settings. However, a single noise point at 5 seconds into the pass was considered valid.

During the pass, the background level was minimal as determined by the processing of the onboard camera frames. However, one disturbance did occur at approximately 5 seconds past the Demonstration start time when a noise signal was registered valid with a DN of 103. Since this signal was detected as stronger than the beacon signal, its coordinates were sent to the tracking algorithm. Luckily, the actual beacon signal was reacquired by the next camera frame 0.01 seconds later, prior to any substantial change in the gimbal pointing. The resulting tracking disturbance was only 1-2 pixels and had minimal impact on the optical link.

Overall, the June 5th, 2014 pass provided a nominal baseline control point against which all other optical downlink passes could be compared to.

5 OFF-NOMINAL ACQUISITION SCENARIOS

Following the successful demonstration of nominal operational scenario, several experimental links were attempted to explore the capabilities of the optical link. These experiments included acquisitions with poor signal-to-noise ratio during low elevation, daytime, and weather-challenged conditions. The results provided important insights into the prevalence of acquisition challenges, such as transient false signals, beacon variability, cloud interruptions, and stray light.

5.1 Daytime acquisition with high threshold

After a number of successful acquisitions, the camera exposure time was generally chosen based on the ground station lighting conditions at the time of the pass. If OCTL was in eclipse, the exposure was typically set to 0.5 milliseconds, whereas for daytime attempts it was usually lowered to 0.2 milliseconds to reduce the overall flux relative to the camera saturation point. The choice of detection threshold, however, was less straightforward since it was sensitive to the time-of-day lighting geometry at the ground station. Final threshold values varied among morning, mid-day, and evening

passes and even an abundance of caution could lead to unintended consequences, as was the case during the June 27 attempt. The 19:04:16 UTC pass meant that the sun was near its highest point in the sky relative to OCTL and a higher-than-normal background flux was anticipated. Therefore, a higher-than-usual centroid threshold of 175 DN was chosen in an attempt to prevent the control algorithm from locking onto noise.

Figure 15 shows an analysis of the data recorded during this pass attempt. At the Demonstration start time, the camera detected the beacon signal and immediately transitioned into closed loop. However, the beacon signal was measured above the threshold of 175 in fewer than half of the camera frames. The result was initially a degraded tracking performance that allowed the beacon to wander several pixels from the tracking target, never achieving steady state. After 7 seconds, the valid beacon points became so sparse that significant gimbal rate errors emerged, eventually driving the beacon off of the CCD focal plane 9.5 seconds into the Demonstration. At 10.5 seconds, the control loop returned to open loop pointing due to the lost beacon. Since the gimbal had diverged significantly from the open loop profile, the sudden acceleration of the transition caused the gimbal to lose pointing calibration. Thus, the beacon was not reacquired in open loop and the pass ended prematurely at 13.75 seconds when a limit switch was unexpectedly triggered. Even if the system had remained in open loop for the remainder of the pass, it is unlikely that the beacon would have been found again since the loss of gimbal calibration would have prevented the gimbal from actually tracking to the BPT.

This attempt became a cautionary tale about the consequences of extreme conservatism. As the last four seconds of data show, the background level was actually very low, ~30 DN (Figure 15, top) despite the high zenith angle of the sun with respect to the ground station. Although this result would have been difficult to anticipate based on prior experience, the threshold of 100 DN that had been previously used would have likely led to a successful pass.

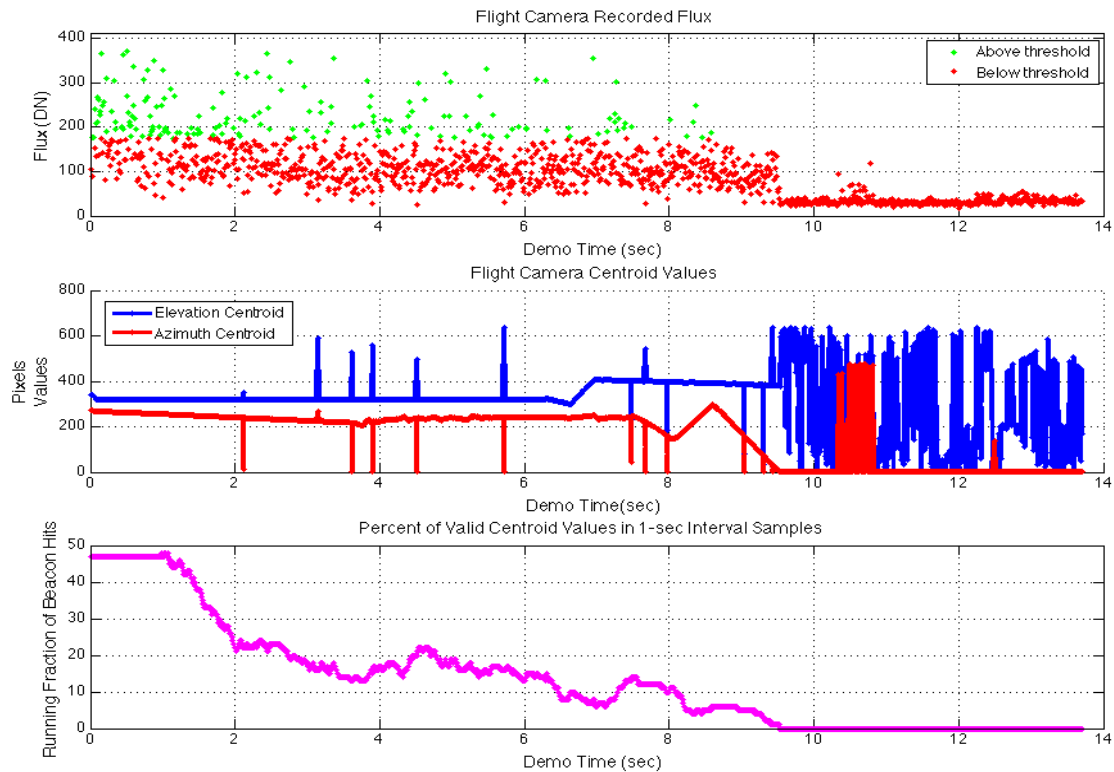


Figure 15: Recorded beacon flux (top), camera centroid coordinates (middle), and beacon validity percentage (bottom) for the 27-JUNE-2014 pass. A conservative, high, threshold prevented the control loop from maintaining lock on a signal that was high enough to provide good tracking had the threshold been set lower.

5.2 Daytime acquisition with low threshold

While a high threshold setting can lead to total beacon loss, a low detection threshold setting can increase susceptibility to background noise disturbances. An excellent example is the 14:09 UTC transmission attempt on July 9. For this

attempt, the camera exposure time was set to 0.2ms and the beacon signal threshold was set to 100 DN. However, due to a high level of upwelling irradiance from the Sun relative geometry, the beacon SNR was on the order of 1 during the planned 25° elevation acquisition. The result was degraded acquisition capability due to several background noise points identified as valid beacon points.

Figure 16 shows the recorded beacon flux and associated beacon validity during the transmission. At first glance, the choice of beacon threshold seems appropriate, as a large majority of the recorded values were considered valid. However, several of the valid points represent noise disturbances with flux values on the order of 100-130 DN rather than the beacon signal. This is clearly evident by examining the calculated centroid values in Figure 17. During the first 40 seconds of the pass, the acquisition algorithm struggles to distinguish the beacon from the background irradiance. The valid centroid value alternates between the real beacon located within 50 pixels of the (240, 320) target and noise artifacts in the lower left quadrant of the camera. Luckily, the true beacon signal composed the majority of valid points, so the noise artifacts were never fully tracked to the center of the camera CCD. Instead the true beacon was perturbed up to 50 pixels during the first 40 seconds, resulting in a delayed optical link acquisition. As the link range decreased, the false signal eventually exited the field of view.

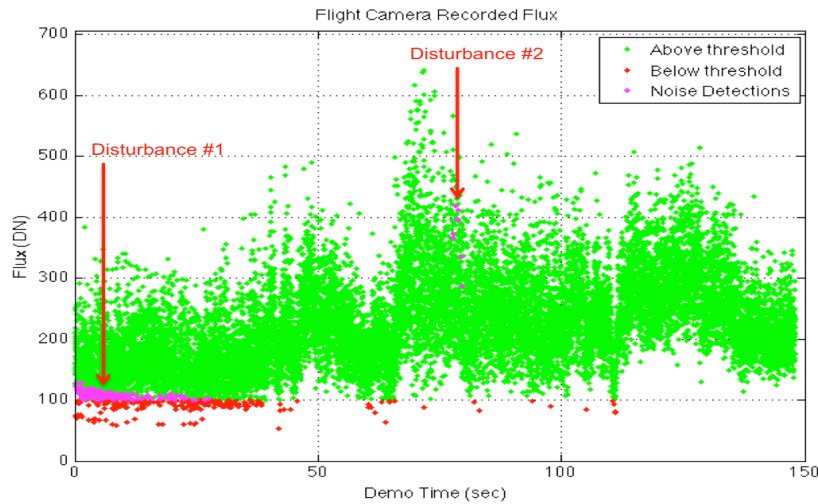


Figure 16: Beacon signal flux for the 09-JUL-2014 pass. A persistent, but weak disturbance during the first 40 seconds degraded closed loop tracking. A brief, but strong disturbance appeared 77 seconds into the pass.

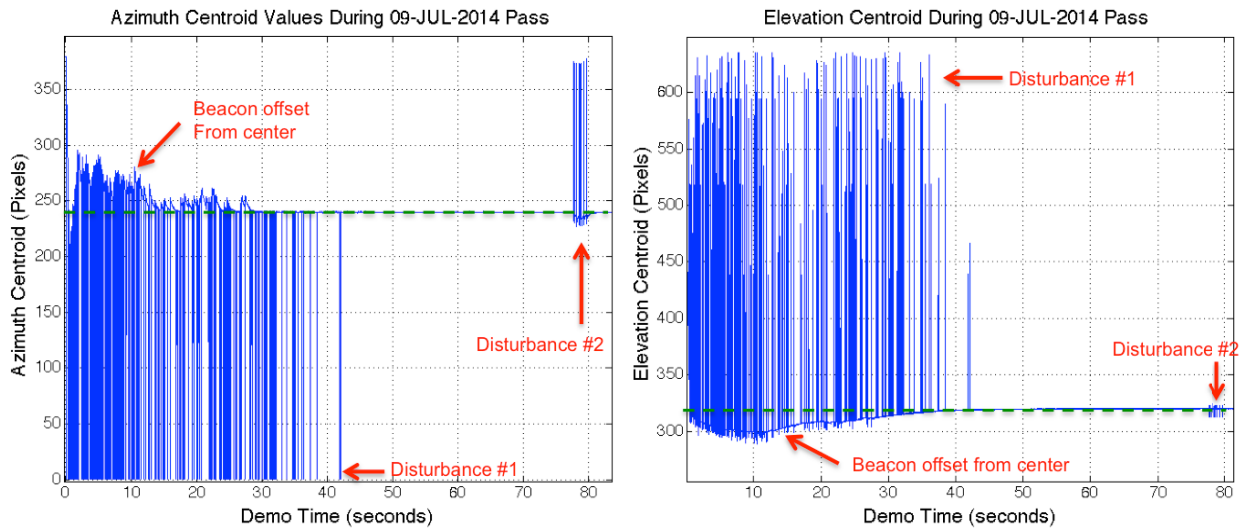


Figure 17. Azimuth (left) and elevation (right) 100 Hz centroid values for 09-JUL-2014 pass. A persistent noise source causes the beacon to be off-pointed up to 50 pixels during the first 40 seconds. A second disturbance causes a brief offset of 2-3 pixels.

A second disturbance occurred approximately 77 seconds into the transmission. Unlike the first disturbance, this one was a relatively brief but focused disturbance with a flux on the order of 400 DN. It appeared for approximately 3 seconds about 130 pixels from the OCTL beacon, almost entirely dispersed along the azimuth axis. As with the first disturbance, the tracking algorithm did not converge on the false signal and only dispersed the true beacon a few pixels from the camera center. This can be explained by the fact that nearly all of the false signal readings were isolated and not recorded in consecutive 100Hz camera frames. The strength of the false signal was sufficient enough to eclipse the beacon threshold and the faintest of the true beacon recordings. However, due to the short-term variability of the beacon flux, consecutive readings were rarely both below the false signal irradiance.

Examination of individual camera frames confirms the presence of structured false signals during the transmission. Two selected images showing both the OCTL beacon and the false signals are shown in Figure 18. The first false signal, identified in the left image, is an extended object measuring almost 100 pixels across that could be reflections from a cloud or ground terrain features. The second false signal, identified in the right image, is a focused object measuring only a few pixels across that could possibly be a temporary glint off of a surface feature. The first false signal could have easily been discarded by a threshold setting of 130 DN or higher, but the second false signal is more concerning since it is similar in structure to the OCTL beacon and entirely dispersed along the direction of ISS motion. For this disturbance, a persistence check would be beneficial to only validate signals that are observable over several consecutive frames.

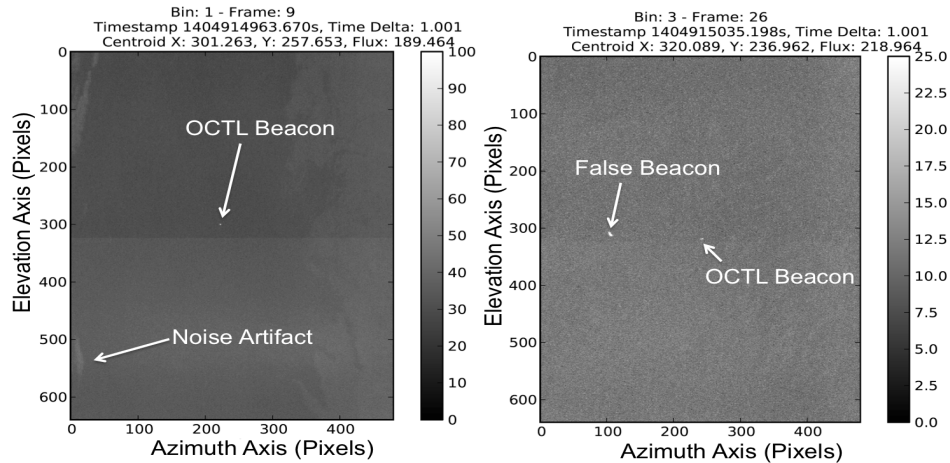


Figure 18: OPALS camera images of optical disturbances during 09-JUL-2014 pass. The first disturbance (left) was diffuse and persistent, while the second disturbance (right) was strong and transient.

A second cautionary tale involves acquisition during partly cloudy conditions. During an August 19th attempted transmission to the German Aerospace Center’s (DLR) optical ground station in Oberpfaffenhofen, Germany, clouds were encountered at the planned 25° acquisition time. The threshold for this pass was set to 75 due to weak beacon observations on a previous DLR pass. Figure 19 shows the observed beacon flux and commanded elevation axis velocity profile during the pass.

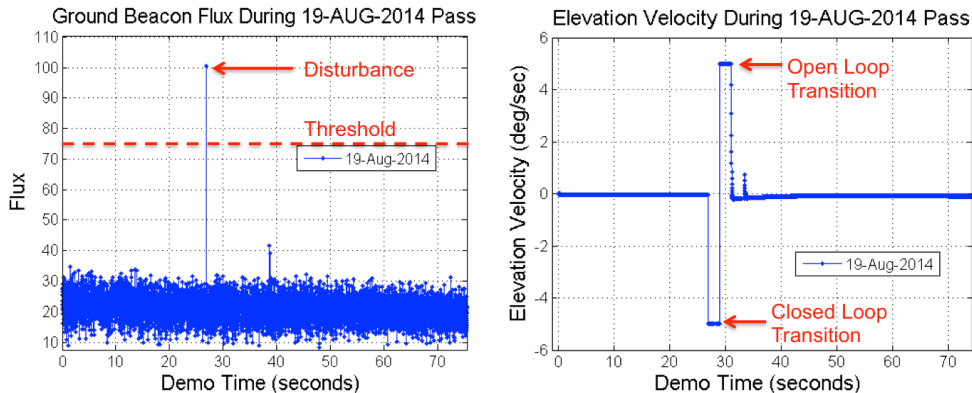


Figure 19: Ground beacon flux (left) and elevation commanded velocity (right) during a 19-AUG-2014 pass with DLR.

At the Demonstration time, the beacon was completely blocked by clouds and the FS remained in open loop pointing, waiting for an opening in the clouds. Before the beacon could be observed, a single camera frame recorded a disturbance at 101 DN. This caused the FS to enter closed loop tracking, followed by a transition to closed loop tracking 2 seconds later. The rapid accelerations in the elevation axis caused the gimbal to lose pointing calibration. The gimbal was off-pointed by about 10° for the remainder of the pass and had no chance of acquiring the beacon during gaps in the clouds. Another pass with partly cloudy conditions, referenced in Figure 7, successfully reacquired twice following cloud interruptions, primarily because false disturbances were not recorded above the beacon threshold.

5.3 Reacquisition following false beacon disturbance

Unlike the false signals encountered during the July 9 transmission, the July 1 pass at 10:26am PDT detected a disturbance several times more intense than beacon signal. The disturbance occurred approximately 75 seconds after the transmission start and was composed of two separate flashes, one lasting 1.25 seconds and one lasting 0.5 seconds. Examination of Figure 20 clearly shows a disturbance with a peak flux of 2200 dwarfing the average beacon flux of 600. The disturbance was observed in consecutive frames throughout the entire first flash, and then alternates with the beacon during a portion of the second flash. Since this disturbance is observed in many consecutive frames, a persistence check would not effectively distinguish the beacon. Based on inspection of the flight camera image shown on the right of Figure 20, this disturbance was likely caused by a glint off of a roadway or waterway, possibly the California Aqueduct.

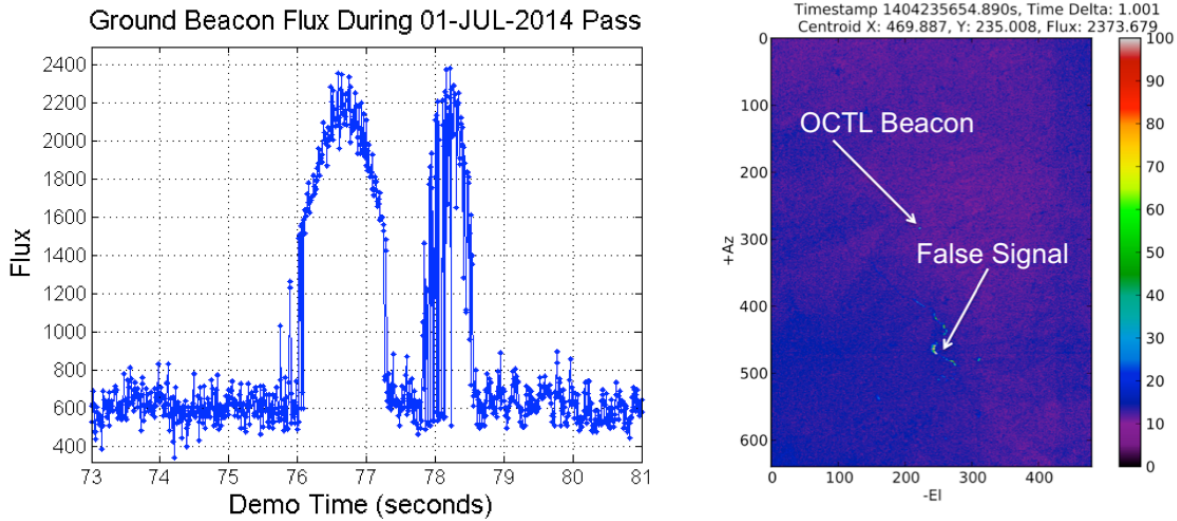


Figure 20: Beacon flux (left) and flight camera image (right) during 01-JUL-2014 pass disturbance.

The disturbance was identified approximately 80 pixels to the left (azimuth) and 180 pixels below (elevation) the camera center. Due to the persistence of the disturbance, the tracking algorithm attempted to acquire the false signal, resulting in a beacon displacement of nearly 90 pixels. Figure 21 depicts the acquisition attempts associated with the disturbance flashes. The first flash is identified with an azimuth coordinate of 160 and steered to approximately 245 during the first acquisition attempt.

Once the first flash dissipates, the beacon is found at an azimuth coordinate of 330 and steered back towards the center until the second flash appears at an azimuth coordinate of 200. This second flash appears to be only 20 pixels displaced from the beacon in azimuth, indicative of an entirely new signal. This signal is tracked for approximately 0.5 seconds until the beacon is reacquired and drawn back to the camera center.

It should be noted that while the azimuth axis chased after the false signals, the elevation axis moved very little. This can be attributed to the shorter time constant on the azimuth control system, since this axis is aligned with the ISS motion and requires faster response times compared to the elevation axis.

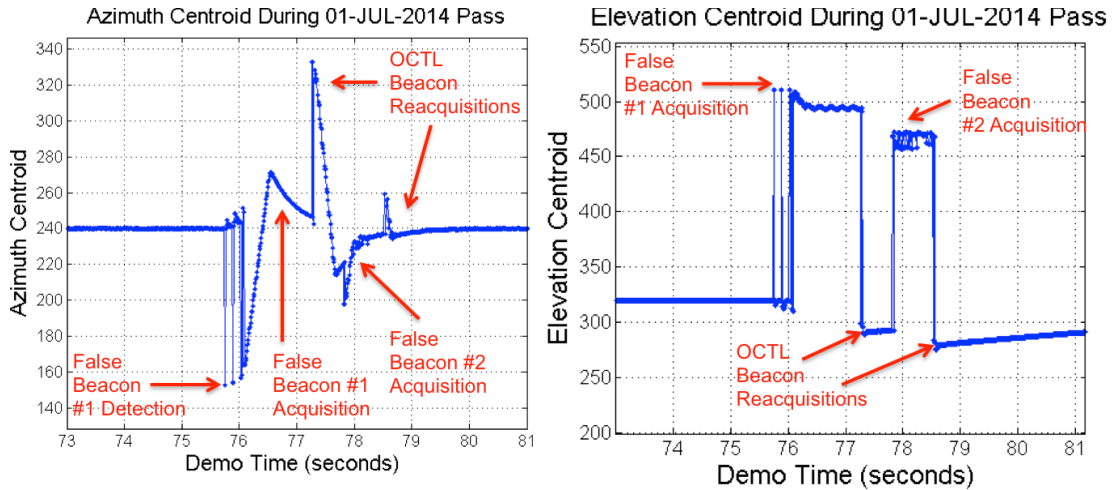


Figure 21: Azimuth (left) and elevation (right) centroid values during 01-JUL-2014 pass. Due to the strength of the disturbance, it was tracked by the control algorithm, resulting in a beacon displacement of nearly 100 pixels.

5.4 Acquisition challenges with weak beacon signal

In addition to optical disturbances, the acquisition process can also encounter challenges from a weak or inconsistent beacon signal. A low elevation acquisition was attempted on June 23 at 03:59 UTC with the Demonstration start time correlated with the 0° elevation rise. The plan was to observe the beacon profile during approach to OCTL and lock on once the beacon exceeded the detection threshold. As Figure 22 illustrates, the beacon did not become detectable until approximately 70 seconds into the pass, at an elevation of 5° and a range of 2100km from OCTL.

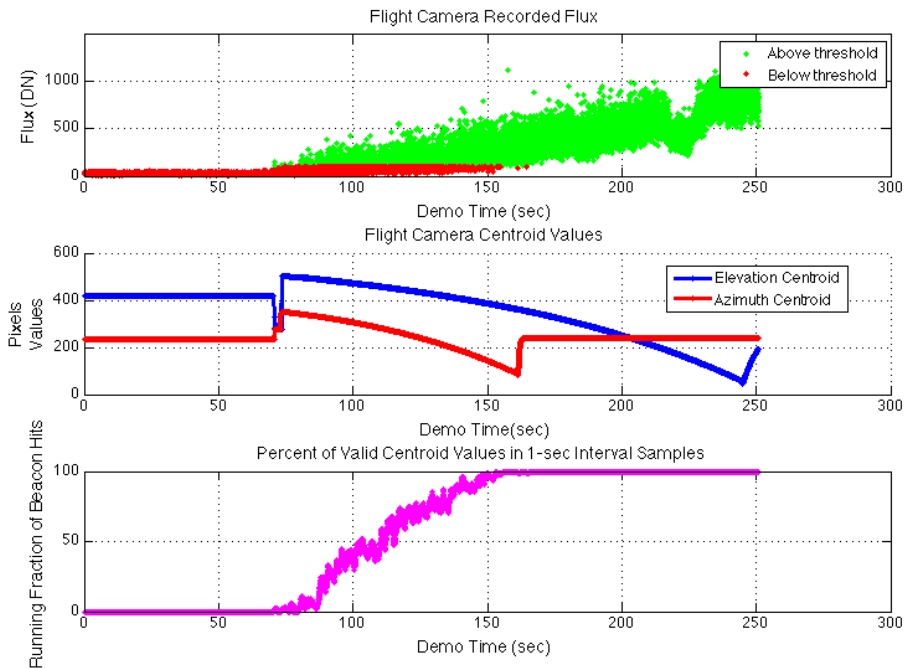


Figure 22: Beacon flux (top), centroid pixel coordinates (middle), and percent of valid beacon hits (bottom) for 23-JUN-2014 pass. Rapid switching between open and closed loop resulted in an integral error buildup the exceeded gimbal correction limits.

Shortly after first detection, a few beacon points exceeded the threshold of 100 DN and the FS entered closed loop tracking. However, since less than 10% of the beacon points were valid, the FS twice transitioned back to open loop

tracking when the beacon was below the threshold for more than 2 seconds. The sudden switching between open loop and closed loop caused loss of pointing calibration, resulting in the beacon being displaced over 100 pixels from the target. At 80 seconds past the Demonstration time, the control algorithm was unable to correct such large errors with less than 10% of the beacon points registered as valid. The result was an integral error buildup that caused the controller to compute velocity changes that exceeded the limitations of the gimbal. The gimbal remained motionless and the beacon motion seen between 80 seconds and 160 seconds was solely due to the ISS orbital motion. At 160 seconds, the azimuth integral error was reduced sufficiently to allow tracking, while the elevation integral error was not fully “unwound” until 240 seconds past the Demonstration time. A proposed solution to both the loss of calibration and gimbal stall issues is an enforcement of acceleration limits within the gimbal feedback controller. However, this solution introduces its own acquisition issues, as discussed in section 5.6.

A symmetrical case occurred during a September 19 attempted transmission to the DLR optical ground station. During this attempt, a strong beacon acquisition was observed at the planned 45° elevation angle and 100% of camera frames reported a valid beacon. However, as Figure 23 illustrates, the beacon signal gradually became fainter, either due to partial cloud occultation or beacon pointing issues. After 14 seconds, the beacon was fully lost and the FS began tracking noise for the remainder of the activity. Eventually, the gimbal contacted a limit switch, ending the Demonstration after 18 seconds.

On a similar July 21 OCTL pass, the ISS was yawed 180° from its nominal attitude and the reverse geometry dictated a higher-than-normal 58° elevation acquisition on approach. The geometry also provided unrestricted line of sight during the departure leg to the northeast. A strong beacon acquisition was observed due to the closer range and the optical link was maintained until 8° elevation on the departure leg. These examples illustrate the importance of a strong beacon signal at the acquisition start. While the June 23 pass never obtained beacon lock, in these two examples pointing lock was maintained until fewer than 20% of beacon points were valid.

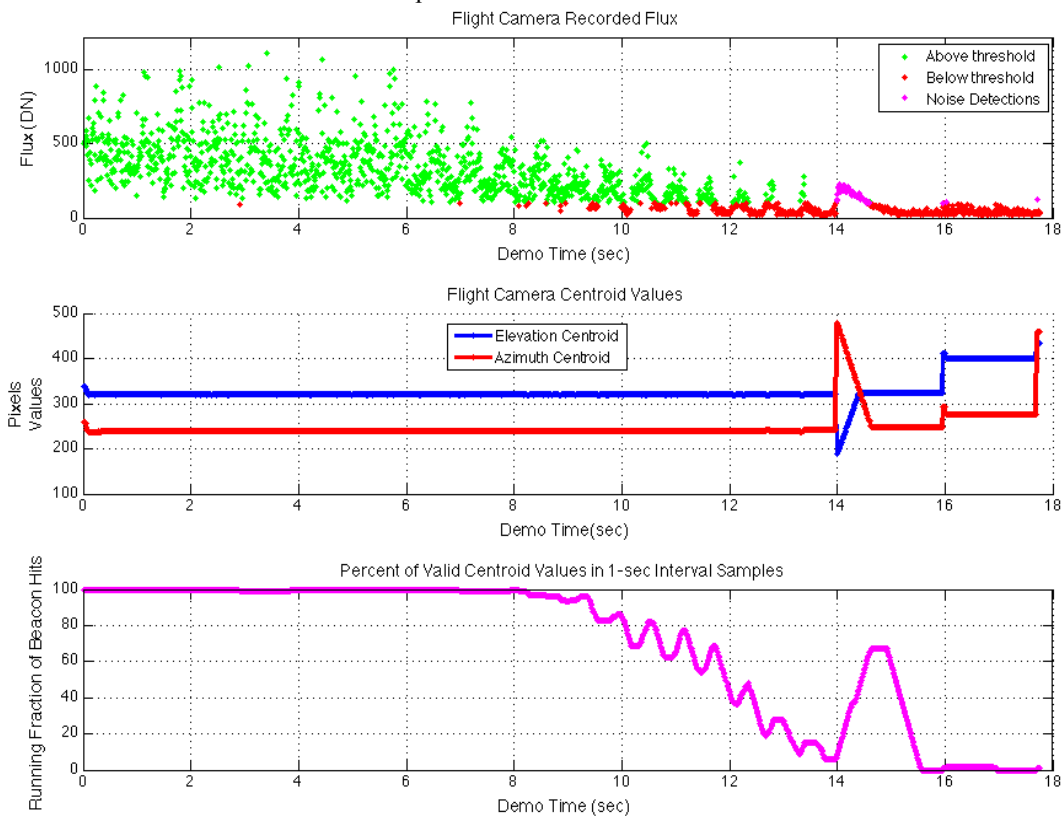


Figure 23: Beacon flux (top), centroid pixel coordinates (middle), and percent of valid beacon hits (bottom) for 19-SEP-2014 pass with DLR. A fading beacon resulted in lock onto a noise source after 14 seconds.

5.5 Stray light issues

On September 9th, 2014 OPALS attempted an optical downlink to the European Space Agency's ground station in Tenerife, Canary Islands. Unfortunately, the optical downlink was unsuccessful. Post activity assessments of the telemetry indicate that stray light from the rising Sun (above the horizon) washed out the ground station's beacon signal during acquisition. Approximately three minutes prior to the planned acquisition, a strong signal was recorded on the OPALS camera as the Sun rose above the Earth's limb. At the acquisition time, the beacon was visible on the onboard OPALS camera, but only a portion of the samples were of higher intensity than the stray sunlight, which registered a flux of 200 DN. The rapid switching between the beacon and stray light signals led to a gimbal stall similar to the phenomena reported in section 5.4. As shown in Figure 24, due to this stray sunlight disturbance, OPALS was unable to achieve pointing lock with Tenerife ground station and lost the beacon entirely after approximately 21 seconds as the ISS orbital motion moved it off of the camera focal array. On a separate September 5 attempt, a closed loop track was maintained with the Tenerife ground station for 54 seconds with additional experiments planned for the future.

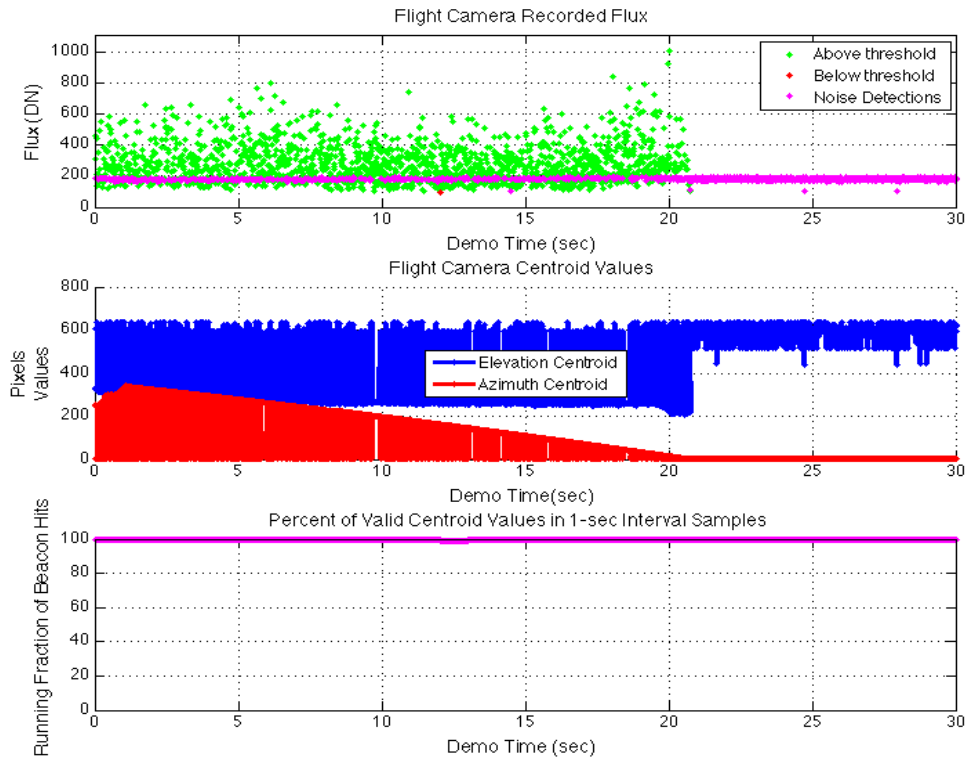


Figure 24: Beacon flux (top), centroid pixel coordinates (middle), and percent of valid beacon points (bottom) for 09-SEPT-2014 pass with ESA ground station. A consistent stray light disturbance above the beacon threshold prevented beacon lock.

5.6 Acceleration limit considerations

A proposed solution to the gimbal stall and pointing calibration issues was to enforce acceleration limits on the calculated control loop velocity corrections. Although the gimbal velocity was already limited to $\pm 5^\circ/\text{s}$, a commanded change from $-5^\circ/\text{s}$ to $+5^\circ/\text{s}$ in one camera frame interval could exceed the limits of the gimbal. The new acceleration limit capability was tested during a DLR pass on October 14 following completion of the prime mission. Using the existing control loop gains, an acceleration limit of $25^\circ/\text{s}^2$ was enforced by the gimbal controller. This resulted in a substantial lag introduced into the control loop tracking performance, contributing to an integral error buildup. As Figure 25 shows, repeated overshoots of the target were observed, resulting in 17 separate transitions between open loop and closed loop. The beacon was reacquired on each transition with no loss of calibration observed. While this enhancement successfully eliminated the calibration and stall issues, further adjustment of the control loop gains will be necessary to improve tracking performance.

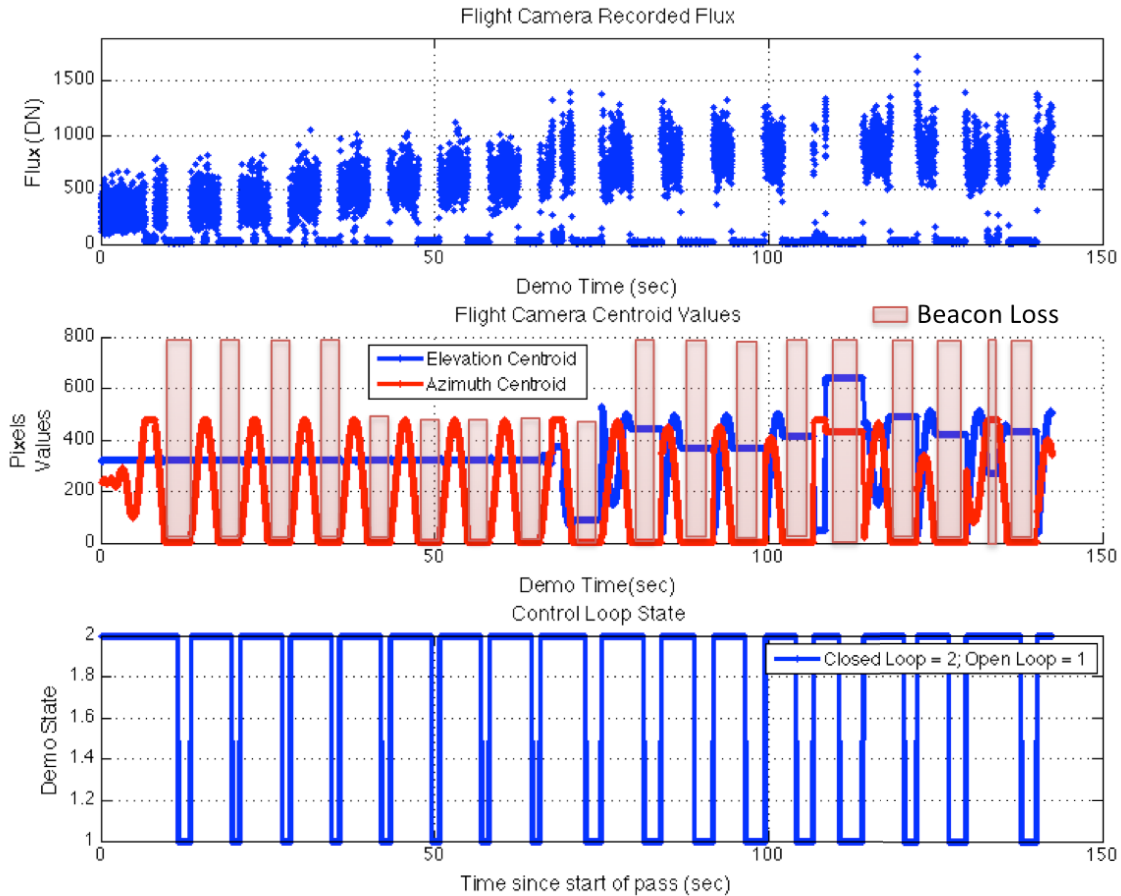


Figure 25: Beacon flux (top), centroid pixel coordinates (middle), and tracking state (bottom) for 14-OCT-2014 pass with DLR. While acceleration limits prevented loss of pointing calibration, a lag was introduced that caused repeated overshoots of the target.

6 CONCLUSION

Including the nominal acquisitions, a total of 18 optical link experiments out of 26 attempts with the OCTL telescope successfully demonstrated closed loop tracking using a ground-based laser beacon, including 9 at night and 9 during the day. While the night passes demonstrated robust acquisition at 25° elevation, several challenges arose for daytime, low elevation, and weather-challenged acquisitions. A fixed beacon detection threshold was custom chosen for each pass to filter out background noise from the ground station beacon signal. Generally, OPALS operational experience showed that a high detection threshold is more likely to cause a total transmission loss than a low threshold due to tracking rate issues. Optical disturbances to the beacon acquisition system were observed to be both focused and highly transient as well as extended and persistent within the camera CCD. While these disturbances generally caused brief transmission interruptions, OPALS demonstrated a capability to reacquire the beacon following losses.

Overall, this demonstration showed that optical communications are practical and repeatable. Even with a simple acquisition and tracking algorithm, a majority of transmission attempts were successful. The bistatic flight design was sufficient to maintain alignment of the uplink and downlink paths to a few hundred microradians. Future enhancements to the image processing algorithm (e.g. beacon shape matching, persistence) and the control algorithm (e.g. acceleration limits, actuator encoded feedback) are likely to make acquisitions more robust in the future.

ACKNOWLEDGEMENTS

The authors express their appreciation to all OPALS team members, past and present, for their dedication and relentless hard work, as well as to the many interns whose contributions have outgrown and outlasted the relatively small time spent with the project. The authors acknowledge all of the OPALS team members, whose technical contributions made the writing of the paper possible.

The work described in this paper was carried out at the Jet Propulsion Laboratory, California Institute of Technology, under a contract with the National Aeronautics and Space Administration.

REFERENCES

- [1] Abrahamson, M., Sindiy, O., Oaida, B., Fregoso, S., Bowles-Martinez, J., Kokorowski, M., Wilkerson, W., and Konyha, A., "OPALS: Mission System Operations Architecture for an Optical Communications Demonstration on the ISS," SpaceOps 2014 13th International Conference on Space Operations, Pasadena, CA, 5-9 May 2014. AIAA-2014-1627.
- [2] Oaida, B.V.; Kokorowski, M.; Erkmen, B.I.; Andrews, K.S.; Wu, W.; Wilkerson, M., "Impact of pointing performance on the optical downlink for the Optical PAYload for Lasercomm Science (OPALS) system" Proc. ICSOS 2014, S3-1, Kobe, Japan, May 7-9 (2014).
- [3] Oaida, B.V.; Wu, W.; Erkmen, B.I.; Biswas, A.; Andrews, K.S.; Kokorowski, M.; Wilkerson, M., "Optical link design and validation testing of the Optical Payload for Lasercomm Science (OPALS) system," *Proc. SPIE 8971*, Free-Space Laser Communication and Atmospheric Propagation XXVI, 897131 (February 2014).
- [4] Oaida, B.V.; Abrahamson, M.J.; Witoff, R.J.; Martinez, J.N.B.; Zayas, D.A., "OPALS: An optical communications technology demonstration from the International Space Station," *Aerospace Conference, 2013 IEEE* , vol., no., pp.1,20, 2-9 March 2013.
- [5] Nimon, J., Smith, S., "'Hello World!' NASA Beams Video from Space Station via Laser," NASA, 6 June 2014, http://www.nasa.gov/mission_pages/station/research/news/opals_beams_video/.
- [6] Hornyak, D. M., *A Researcher's Guide to International Space Station (ISS) Technology Demonstration*, NASA ISS Program Science Office, NASA Johnson Space Center, Houston, TX, July 2013, pp. 1-45.